Cation disorder as the major electron scattering source in crystalline InGaZnO

Youngho Kang, Youngmi Cho, and Seungwu Han

Citation: Appl. Phys. Lett. **102**, 152104 (2013); doi: 10.1063/1.4802093
View online: http://dx.doi.org/10.1063/1.4802093
View Table of Contents: http://apl.aip.org/resource/1/APPLAB/v102/i15
Published by the American Institute of Physics.

Cation disorder as the major electron scattering source in crystalline InGaZnO

Youngho Kang,[1] Youngmi Cho,[2] and Seungwu Han[1,a)]
[1]*Department of Materials Science and Engineering and Research Institute of Advanced Materials, Seoul National University, Seoul 151-755, South Korea*
[2]*CAE Team, Samsung Display Co., Ltd, 95 Samsung 2-ro, Giheung-gu, Youngin-City, Gyeonggi-Do 446-711, South Korea*

(Received 14 December 2012; accepted 3 April 2013; published online 15 April 2013)

We theoretically investigate the electron transport mechanism in crystalline In-Ga-Zn oxides using the semi-classical transport theory. The site disorder of Ga and Zn atoms is treated based on the virtual crystal approximation. The valence difference between Ga^{3+} and Zn^{2+}, modeled by screened Coulomb potential, plays a critical role in determining the total electron mobility. The temperature and carrier-density dependences of the calculated electron mobility are in excellent agreement with experimental data. The unusual behavior of electron mobility is explained based on the energy-dependent relaxation time and underlying band structure. © *2013 AIP Publishing LLC* [http://dx.doi.org/10.1063/1.4802093]

Since Nomura *et al.*[1] reported fabrication of the transparent thin-film transistor (TFT) using the single-crystalline $InGaO_3(ZnO)_5$ channel layer, the interest in In-Ga-Zn-O (IGZO) material system has been growing rapidly.[2–5] In addition, the amorphous phase of IGZO shows an electron mobility comparable to that of the crystalline phase,[6,7] enabling the material to replace *a*-Si as the active layer in TFTs used in the state-of-the-art flat panel display.[6,8,9]

The electron mobility is a key performance metric of IGZO used in TFTs. As such, understanding electron scattering mechanism is important to optimize the material composition toward higher electron mobility. The electron mobility of crystalline (*c*-IGZO) or amorphous (*a*-IGZO) IGZO is about $\sim 10\,cm^2/V \cdot s$, which is significantly larger than for typical amorphous materials but still one order below those of crystalline Si or binary conducting oxides. The main limiting factor against higher electron mobility is thought to be site (in *c*-IGZO) or structural (in *a*-IGZO) disorders.[10]

Experimentally, it was found that increasing carrier concentration or temperature enhances the electron mobility in *c*- and *a*-IGZO.[10] This is in contrast with typical semiconductors like Si for which the mobility is reduced at large carrier densities or high temperatures due to further scattering by ionized impurities or phonons, respectively. Furthermore, the temperature dependence of electron mobility is weakened at high concentrations ($\sim 10^{19}\,cm^{-3}$).[11] Explaining on these unique transport behaviors would be critical to identify the major scattering mechanism.

So far, two models have been proposed about the disorder effect on electron mobility. Kamiya *et al.* suggested a percolation model in which conducting electrons flow along the low-energy path in the random potential surface induced by disorder in *c*- or *a*-IGZO.[10,11] On the other hand, Tomai *et al.* proposed a hopping model to explain the electron mobility in *a*-IGZO. In this model, electrons are localized between potential barriers and thermally hop between low-energy sites.[12] While these models reasonably account for the temperature and carrier dependence of electron mobility, their phenomenological nature prohibits more quantitative and predictive analysis. In this Letter, we try to evaluate the electron Hall mobility in *c*-IGZO, considering full electronic structure and various scattering mechanisms. The site disorder in *c*-IGZO, i.e., random occupation of Ga and Zn in GaZnO layers is considered within the virtual crystal approximation (VCA)[13] that was applied to studying electron mobility in Si_xGe_{1-x}.[14]

Among various compositions of *c*-IGZO, $InGaZnO_4$ (IGZO1) has been extensively studied and we focus on this compound in the present study. [The results on $InGaO_3(ZnO)_5$ (IGZO5) are provided as a supplementary material.[15]] The density-functional theory (DFT) calculations to obtain electronic structure and material parameters are performed with VASP[16] using the same computational setup as in Ref. 17. The crystal structure of IGZO1 is shown in Fig. 1(a) where InO and GaZnO layers alternate along the *c*-axis. The key structural feature is that Ga and Zn atoms randomly occupy the same crystallographic sites in GaZnO layers, introducing randomness in the crystal structure. This structural disorder also applies to other stoichiometric compositions of $InGaO_3(ZnO)_n$.[11]

To examine the influence of site disorder on the electronic structure, we expand the unit cell of IGZO1 to include 48 formula units of $InGaZnO_4$ and randomly distribute Ga and Zn atoms over cation sites in GaZnO layers. Figure 1(b) shows the density of states (DOS) and inverse-participation ratios (IPRs)[18] near the Fermi level. Roughly speaking, IPR is equal to $1/N$ if the state is distributed uniformly over N atoms. It is noted in Fig. 1(b) that IPRs for the states near the valence band maximum show relatively large values in comparison with other states. This implies that the valence-top states are strongly affected by the cation disorder and localized over a few oxygen atoms. In contrast, IPRs for the states near the conduction bottom remain to be small values as in the ordered crystalline structures. This is attributed to the metal-*s* character of the states near the conduction band edge, which is insensitive to angular disorder.[17,19] While one

a)Electronic mail: hansw@snu.ac.kr

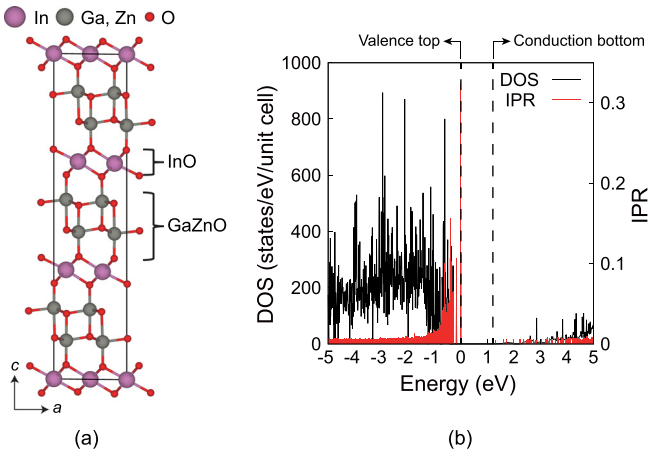

FIG. 1. (a) Crystal structure of $InGaZnO_4$. The InO and GaZnO layers are alternately stacked along the c-axis. Ga and Zn atoms in GaZnO layer are randomly distributed over cation sites. (b) Electronic DOS and inverse IPR of the $InGaZnO_4$ supercell including 336 atoms.

cannot exclude a possibility that conduction electrons are localized on larger length scales, say, $10 \sim 100$ nm, we assume in this work that electrons are fairly well delocalized in spite of the cation disorder and introduce an electronic band structure characteristic of the periodic potential in investigating electron transport mechanism.

First, we schematically decompose the self-consistent potential of c-IGZO1 [$U(\mathbf{r})$] into a sum of effective potentials contributed by each atom;

$$U(\mathbf{r}) = \sum_{\text{In}} U_{\text{In}}(\mathbf{r} - \mathbf{R}_{\text{In}}) + \sum_{\text{Ga}} U_{\text{Ga}}(\mathbf{r} - \mathbf{R}_{\text{Ga}}) + \sum_{\text{Zn}} U_{\text{Zn}}(\mathbf{r} - \mathbf{R}_{\text{Ga}}) + \sum_{\text{O}} U_{\text{O}}(\mathbf{r} - \mathbf{R}_{\text{O}}), \quad (1)$$

where $\mathbf{R}_\alpha$ represents the position of atom α. We separate $U(\mathbf{r})$, which is aperiodic due to the random distribution of Ga and Zn, into the averaged virtual-crystal potential [$U_{\text{vc}}(\mathbf{r})$] and random potential [$U_{\text{rand}}(\mathbf{r})$];

$$U_{\text{vc}}(\mathbf{r}) = \sum_{\text{In}} U_{\text{In}}(\mathbf{r} - \mathbf{R}_{\text{In}}) + \sum_{\text{O}} U_{\text{O}}(\mathbf{r} - \mathbf{R}_{\text{O}}) + \sum_{\text{Ga/Zn}} \left[f_{\text{Ga}} U_{\text{Ga}}(\mathbf{r} - \mathbf{R}_{\text{Ga/Zn}}) + f_{\text{Zn}} U_{\text{Zn}}(\mathbf{r} - \mathbf{R}_{\text{Ga/Zn}}) \right], \quad (2)$$

$$U_{\text{rand}}(\mathbf{r}) = \sum_{\text{Ga/Zn}} C_{\text{Ga/Zn}} \Delta U(\mathbf{r} - \mathbf{R}_{\text{Ga/Zn}}), \quad (3)$$

$$\Delta U(\mathbf{r}) = U_{\text{Ga}}(\mathbf{r}) - U_{\text{Zn}}(\mathbf{r}), \quad (4)$$

where $\mathbf{R}_{\text{Ga/Zn}}$ indicates cation sites in GaZnO layers and $f_{\text{Ga(Zn)}}$ means the ratio of the number of Ga(Zn) atoms to the total number of Ga and Zn atoms in the system. In Eq. (3), $C_{\text{Ga/Zn}}$ is a random function that depends on the cation type at $\mathbf{R}_{\text{Ga/Zn}}$

$$C_{\text{Ga/Zn}} = \begin{cases} f_{\text{Zn}}, & \text{for } \mathbf{R}_{\text{Ga/Zn}} = \mathbf{R}_{\text{Ga}} \\ -f_{\text{Ga}}, & \text{for } \mathbf{R}_{\text{Ga/Zn}} = \mathbf{R}_{\text{Zn}}. \end{cases} \quad (5)$$

On the other hand, by examining the relaxed structure of the expanded supercell, we confirm that the local geometry is similar between Ga and Zn atoms. Therefore, except for inside the core region, $\Delta U(\mathbf{r})$ is dominated by the Coulomb potential that stems from the valence difference of Ga^{3+} and Zn^{2+} (ΔZ_{eff}), screened by free electrons

$$\Delta U(r) = -\frac{\Delta Z_{\text{eff}} e^2}{4\pi\epsilon_s r} e^{-r/L_s}, \quad (6)$$

where ϵ_s and L_s indicate the static dielectric constant and screening length, respectively. Thus, we introduce a band picture based on $U_{\text{vc}}(\mathbf{r})$ and consider the electronic scattering by $U_{\text{rand}}(\mathbf{r})$ perturbatively.

The scattering by $U_{\text{rand}}(\mathbf{r})$ can be estimated by the first-order Born approximation within an isotropic free-electron model.[20] The scattering rate (or transition rate) from $\mathbf{k}$ to $\mathbf{k}'$ in the momentum space is obtained from the Fermi golden rule;

$$S_{\mathbf{k},\mathbf{k}'} = \frac{2\pi \Delta Z_{\text{eff}}^2 e^4 \rho_{\text{Ga/Zn}} f_{\text{Ga}} f_{\text{Zn}}}{V\hbar\epsilon_s^2 (|\mathbf{k}' - \mathbf{k}|^2 + 1/L_s^2)^2} \frac{2m_{\text{e}}^*}{\hbar^2} \delta(\mathbf{k}'^2 - \mathbf{k}^2), \quad (7)$$

where $\rho_{\text{Ga/Zn}}$ and V are the density of Ga/Zn sites and the volume of the system, respectively. We call this cation-disorder (CD) scattering rate. In addition, we also consider ionized impurity (II) and polar optical phonon (POP) scattering in similar ways.[20]

The Hall mobility (μ) is evaluated from the low-field solution of Boltzmann transport equation considering the Fermi-Dirac distribution and the Hall factor $\langle\tau^2\rangle/\langle\tau\rangle^2$, where $\langle\tau\rangle$ represents the average relaxation time that are obtained independently for II, POP, and CD scattering mechanisms. The material parameters used in the calculation are $m_{\text{e}}^*/m_{\text{e}} = 0.25$, $\epsilon_\infty = 3.99$ (optical dielectric constant), $\epsilon_s = 9.06$, $\hbar\omega_{\text{op}} = 69.70$ meV (optical phonon energy), and $\Delta Z_{\text{eff}} = 0.3$. All parameters are obtained by DFT calculations except for ΔZ_{eff}, which was selected to produce the best agreement with the experimental data but close to the Bader-charge difference of 0.4.[21] We consider a singly ionized impurity model for II scattering.

Figure 2(a) shows the temperature dependence of the computed Hall mobility. It is seen in Fig. 2(a) that the Hall mobility is mainly limited by the CD scattering over the given temperature range, and the total mobility ($1/\mu = 1/\mu_{\text{POP}} + 1/\mu_{\text{II}} + 1/\mu_{\text{CD}}$) is almost identical to μ_{CD}. The CD scattering dominates up to 10^{20}cm^{-3}. (As the temperature increases, POP scattering becomes stronger and eventually comparable to CD scattering at ~900 K. However, this is much higher than operation temperatures, $223 \sim 323$ K (Ref. 22).)

In Figs. 2(b) and 2(c), theoretical and experimental Hall mobilities are compared as a function of carrier density and temperature, respectively. The agreements between theory and experiment are excellent. In particular, the main features of the mobility, that is to say, the increase of μ with temperature and carrier density is well reproduced. Figure 2(d) shows the Arrhenius plot of μ at various carrier densities; at low carrier densities, the mobility is sensitive to temperature but the dependence is attenuated at higher carrier densities ($\gtrsim 10^{19}$ cm^{-3}). This is exactly what has been observed in the experiment.[10,11] The quantitative as well as qualitative

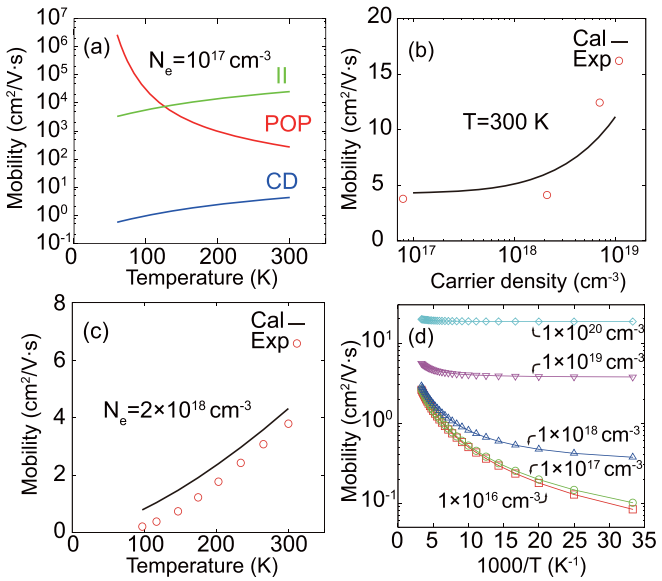

FIG. 2. (a) Theoretical Hall mobility with respect to each scattering mechanism (II: ionized impurity, POP: polar optical phonon, and CD: cation disorder). (b)–(c) The computed (total) Hall mobility and experimentally measured data as a function of (b) carrier density and (c) temperature. (d) Temperature dependence of Hall mobility at various carrier densities.

agreements with experimental data confirm that the main scattering mechanism in *c*-IGZO is the cation disorder. We also computed the mobility of IGZO5, and the agreement with the experiment is at a similar level. (See supplementary information.[15])

In order to explain the above temperature and carrier dependence of the Hall mobility, we examine the energy-dependent relaxation time and carrier distribution at certain carrier densities (see Fig. 3). In Fig. 3(a), the relaxation time for CD scattering is the shortest among the considered mechanisms, which is consistent with the lowest mobility in

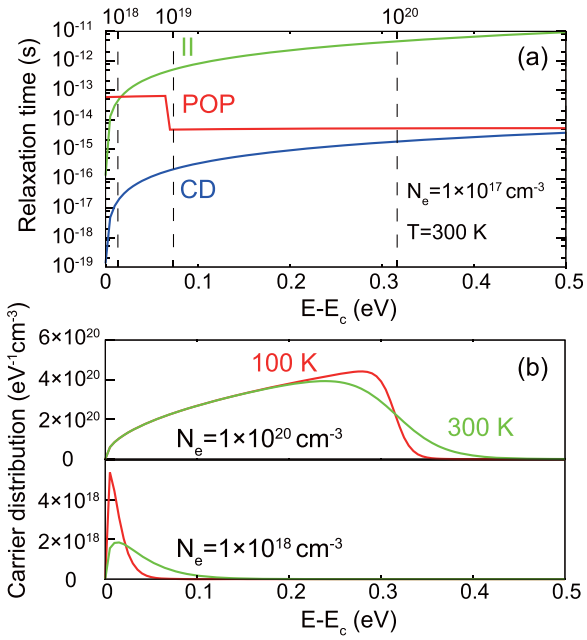

FIG. 3. (a) The relaxation time for each II, POP, and CD scattering mechanisms as a function of the electron energy relative to the conduction bottom (E_c). Vertical lines indicate the Fermi levels at the zero temperature for several carrier densities in cm^{-3}. (b) Carrier distribution over the electron energy.

Fig. 2(a). It is noticeable that the relaxation time of CD scattering increases rapidly at low electron energies and this is the main reason why the mobility increases with the carrier density. (See the zero-temperature Fermi levels at specific carrier densities marked by vertical dashed lines.) In contrast with impurity scattering, the number of scattering source is fixed in CD and, therefore, the increased relaxation time directly results in higher mobilities. The rapid rise of the Fermi level is attributed to the large dispersion and non-degeneracy of the conduction band.

The temperature dependence of mobility found in Figs. 2(c) and 2(d) can also be explained in similar ways; the carrier distribution in Fig. 3(b) shows that the thermally activated electrons occupy higher energy states near the Fermi level, which results in the longer relaxation time, following the foregoing discussion. This accounts for the temperature dependence in Fig. 2(c). At high carrier densities, say $10^{20}\,cm^{-3}$, the thermal activation excites electrons that are ~0.3 eV above the conduction bottom. [See Fig. 3(b)] In this case, the relaxation time in Fig. 3(a) increases rather slowly than in the low-energy region, softening the influence of temperature. In addition, the relative amount of thermally excited electrons are reduced at high carrier densities. These two factors contribute to the weakening of temperature dependence at high carrier densities, as shown in Fig. 2(d).

It would be also intriguing to investigate the effect of varying the degree of CD on the mobility. To this end, we evaluate the Hall mobility of $InGaO_3(ZnO)_n$ with n ranging from 1 to 7 (see Fig. 4). $InGaO_3(ZnO)_n$ is modeled as a layered structure consisting of InO and GaZnO layers for all n values and it is assumed that cations in GaZnO layers are randomly distributed. Such structures are consistent with experiment for $n=1$ and 5.[11] This means that $\rho_{Ga/Zn}$ and $f_{Ga(Zn)}$ in Eq. (7) are changed according to n. The variation in other material parameters is neglected. In Fig. 4, it is found that the Hall mobility at 300 K and carrier density of $10^{18}\,cm^{-3}$ increases monotonically with n. This is due to the reduced degree of CD with the increasing population of Zn atoms. On the other hand, within POP and II scattering mechanisms, the degree of CD mainly affects material parameters such as the effective mass and dielectric constant. With reference to IGZO1, II scattering in IGZO5 ($n=5$ in Fig. 4) is little changed while POP scattering is reduced by a factor 2 at room temperatures. Therefore, the mobility is still significantly limited by CD scattering even at the largest n of 7. Overall, the mobilities of *c*-IGZOs are similar within the given compositional variation, which seems to be consistent with the experimental results in Ref. 23.

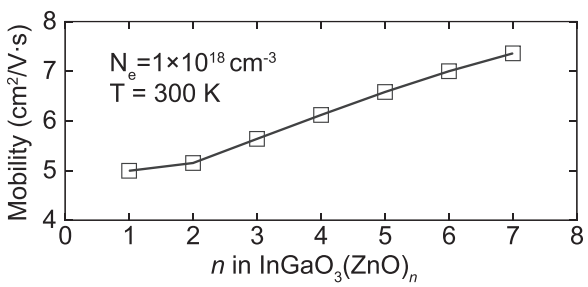

FIG. 4. The Hall mobility determined by CD scattering of IGZO with various composition.

In summary, we evaluated the Hall mobility of electron carriers in *c*-IGZO considering various microscopic mechanisms. In particular, the positional disorder of Ga and Zn was treated within the virtual crystal approximation. The calculated Hall mobility is dominated by cation-disorder scattering and is in good agreement with the experimentally measured data, identifying cation disorder as the major electron scattering source.

This work was supported by Samsung Display and the Pioneer Research Center Program through the National Research Foundation of Korea funded by the Ministry of Education, Science and Technology (2012-0009563). The computations were carried out at KISTI (No. KSC-2012-C3-20).

[1]K. Nomura, H. Ohta, K. Ueda, T. Kamiya, M. Hirano, and H. Hosono, Science **300**, 1269 (2003).
[2]H. Yabuta, M. Sano, K. Abe, T. Aiba, T. Den, and H. Kumomi, Appl. Phys. Lett. **89**, 112123 (2006).
[3]D. Cho, J. Song, K. D. Na, C. S. Hwang, and J. H. Jeong, Appl. Phys. Lett. **94**, 112112 (2009).
[4]K. Kusunoki, M. Kaneyasu, H. Harada, H. Katagiri, K. Moriya, H. Ohnuma, Y. Hirakata, J. Koyama, S. Yamazaki, Y. Shima, and D. Kurosaki, SID Symp. Digest Tech. Papers **43**, 217 (2012).
[5]W.-J. Lee, E.-A. Choi, J. Bang, B. Ryu, and K. J. Chang, Appl. Phys. Lett. **93**, 111901 (2008).
[6]K. Nomura, H. Ohta, A. Takagi, T. Kamiya, M. Hirano, and H. Hosono, Nature **432**, 488 (2004).
[7]A. Suresh, P. Wellenius, A. Dhawan, and J. Muth, Appl. Phys. Lett. **90**, 123512 (2007).
[8]S. Jeon, S.-E. Ahn, I. Song, C. J. Kim, U.-In. Chung, E. Lee, I. Yoo, A. Nathan, S. Lee, J. Robertson, and K. Kim, Nature Mater. **11**, 301 (2012).
[9]J. Lee, D. Kim, D. Yang, S. Hong, K. Yoon, P. Hong, C. Jeong, H. Park, S. Y. Kim, S. K. Lim, S. S. Kim, K. Son, T. Kim, J. Kwon, and S. Lee, SID Symp. Digest Tech. Papers **39**, 625 (2008).
[10]K. Nomura, T. Kamiya, H. Ohta, K. Ueda, and M. Hirano, Appl. Phys. Lett. **85**, 1993 (2004).
[11]T. Kamiya, K. Nomura, and H. Hosono, J. Disp. Technol. **5**, 462 (2009).
[12]S. Tomai, M. Nishimura, M. Itose, M. Matuura, M. Kasami, S. Matsuzaki, H. Kawashima, F. Utsuno, and K. Yano, Jpn. J. Appl. Phys., Part 1 **51**, 03CB01 (2012).
[13]J. W. Harrison and J. R. Hauser, Phys. Rev. B **13**, 5347 (1976).
[14]F. Murphy-Armando and S. Fahy, Phys. Rev. Lett. **97**, 096606 (2006).
[15]See supplementary material at http://dx.doi.org/10.1063/1.4802093 results of IGZO5.
[16]G. Kresse and J. Furthmuller, Phys. Rev. B **54**, 11169 (1996); P. E. Blöchl, *ibid.* **50**, 17953 (1994).
[17]Y. Kang, S. H. Jeon, Y. W. Son, Y. S. Lee, M. Ryu, S. Lee, and S. Han, Phys. Rev. Lett. **108**, 196404 (2012).
[18]E. Cho, Y. Yong, and S. Han, Appl. Phys. Lett. **99**, 183501 (2011).
[19]J. Robertson, Phys. Status Solidi B **245**, 1026 (2008).
[20]B. K. Ridley, *Quantum Process in Semiconductors*, 3rd ed. (Oxford University Press, New York, 1993).
[21]J. L. F. Da Silva, A. Walsh, and S. H. Wei, Phys. Rev. B **80**, 214118 (2009).
[22]K. Hoshino and J. F. Wager, IEEE Electron Device Lett. **31**, 818 (2010).
[23]T. Kamiya, K. Nomura, and H. Hosono, J. Disp. Technol. **5**, 273 (2009).